

Single-particle spectra in bootstrap model based on dual-topological-unitarization diagrams

K. Hirose

Institute of Physics, Teikoku Women's University, Moriguchi 570, Japan

T. Kanki

Institute of Physics, College of General Education, Osaka University, Toyonaka 560, Japan

(Received 31 July 1981; revised manuscript received 11 March 1983)

We study a bootstrap model of inclusive reactions based on dual-topological-unitarization diagrams of the multi-Regge type. By applying the bootstrap equations developed for the multifireball model, we are able to calculate the branching process of the dual multi-Regge chain, keeping longitudinal-momentum conservation exactly. We calculate various single-particle spectra in pion, kaon, and proton fragmentation. These spectra are compared with experimental data.

I. INTRODUCTION

For small- p_T multihadron production, many features in the central region have been well understood in the framework of the dual-topological-unitarization (DTU) model^{1,2} and its modified versions.³ On the other hand, recent experiments have shown that in the fragmentation region, the free-parton picture, associated with the recombination model,⁴ works very well.⁵ Although we write quark lines in the DTU model, the quarks are not free; the string assumed implicitly by the duality carries momentum from one quark line to another. It is therefore interesting to find predictions by the DTU model in the fragmentation region.

In the so-called dual sheet model,³ discussed frequently in the last few years, one assumes jet universality. Then internal consistencies among fragmentation spectra in various reactions, including hard jets, have been studied. In this model, no clear prescriptions have yet been found to calculate the fragmentation spectra directly from the basic idea of the model. On the other hand, in the DTU model of multi-Regge type,^{1,2} it is in principle possible to get the definite predictions in the fragmentation region, because the strong-ordering condition under the multi-Regge hypothesis is sufficient to determine the fast-particle spectra. Unfortunately, this is a practically very difficult task because it is hard to accommodate momentum conservation, which is vital for dealing with fast-particle production.

In this paper, we will study a model which closely resembles the DTU model of the one-dimensional multi-Regge type and which is hereafter called the dual multi-Regge bootstrap (DMB) model. The two models are the same in the basic idea and are described by the same quark-line (DTU) diagrams. But in the DMB model, we use a technique based on the Mueller-Regge formalism and somewhat different from the conventional rapidity formalism. This technique was given several years ago as the bootstrap equation for the multifireball model.^{6,7} The (longitudinal-) momentum conservation is then satisfied exactly, but the strong-ordering condition works only in the average. In this paper, we restrict ourselves to the

one-dimensional model in treating the bootstrap equation. Otherwise we encounter untractable complexity. We will consider the standard DTU diagram (Fig. 1), where the highest (exchange-degenerate) meson trajectories are considered as exchanged Reggeons. Possible baryon exchanges are neglected since they will not be dominant processes and they cause too much complications in the formalism. We shall calculate in this model various inclusive meson spectra for π - p or K - p reactions over all regions of the fractional momenta ($0 \leq |x| \leq 1$).

The technique of this bootstrap equation was already applied to models of the Chew-Pignotti type,⁷ but the result obtained was rather trivial, because no flavor dependence was introduced in this type of model. On the other hand, in the DTU diagrams, the flavor of the incident hadron is carried along the quark lines and can give non-trivial effects to various fragmentation spectra. We are most interested in extracting these effects, since so far it has not been discussed satisfactorily in the framework of the multi-Regge model.

In Sec. II, we shall describe the bootstrap formalism of the dual multi-Regge (DM) chain. The role of the valence quarks is manifested. The flavor dependence and indirect production through resonance decays are discussed in Sec. III. Section IV is devoted to the discussion of the predicted spectra of the DMB model, and Sec. V to the summary. The pion, kaon, and proton fragmentations are treated and some expressions are given in the Appendix.

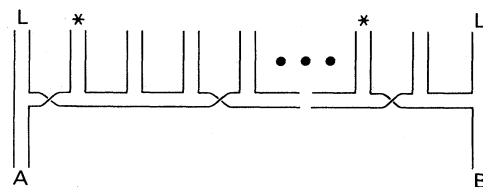


FIG. 1. The DM chain (the Pomeron sector). In the Reggeon sector, all internal Reggeons are uncrossed.

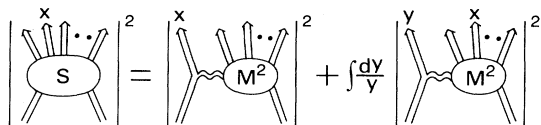


FIG. 2. The schematic illustration of the integral equation (1).

II. THE BASIC EQUATIONS OF THE DMB AND ITS SOLUTION

The method we employ here is based on the bootstrap integral equation^{6,7} on the normalized single-particle inclusive distribution,

$$n(x) \equiv (1/\sigma^{\text{inel}}) \int dP_1^2 E(d\sigma/d^3P),$$

where x is the fractional momentum. Consider the meson-meson collision. Then we get the following equations for the DMB model, by applying the argument in Ref. 7:

$$n^{(i)}(x) = n_L^{(i)}(x) + \int_0^{1-x} \frac{dy}{y} n_L^{(i)}(y) n^{(i)} \left[\frac{x}{1-y} \right] \quad (i = T, R), \quad (1)$$

where T and R indicate the total sector (whole contributions) and the Reggeon sector (see Fig. 1), respectively. For the time being, we ignore the quark flavors. Only the region $x > 0$ is considered, the region $x < 0$ can be similarly treated.⁷ We illustrate Eq. (1) schematically in Fig. 2. $n_L(x)$ corresponds to the first term of the right-hand side of this schematic equation and represents the leading-particle distribution. The leading particle means the particle emitted from the end vertex. $n_L(x)$ must satisfy the normalization condition

$$\int_0^1 (dx/x) n_L^{(i)}(x) = 1, \quad (2)$$

which shows that there is one and only one leading particle. This relation restricts, by combining with (1), all internal branching processes to be two-body (virtual) decays.

Before going into detail, we shall give some general remarks.

(a) In deriving (1) we have to provide⁷ all multi-Regge amplitudes given by arbitrary permutations on momenta of outgoing particles. But dominant contributions come from the configurations satisfying the canonical strong ordering of outgoing momenta. In fact, condition (2) can be satisfied only if $n_L(x) \rightarrow 0$ for $x \rightarrow 0$, and the faster decrease of $n_L(x)$ here corresponds to the larger suppression of noncanonical amplitudes. When $x \rightarrow 1$, the integral term in (1) is clearly noncanonical and vanishes by this property of n_L . Further, this term corresponds to the sum, $n_L \otimes n_L + n_L \otimes n_L \otimes n_L + \dots$ [the iteration series for (1)], in which every term is dominated by the integration domain where all n_L 's have their arguments to be large. This domain corresponds to the canonical strong-ordering configurations.

(b) The integral equation (1) incorporates conveniently the different Mueller-Regge diagrams working in the dif-

ferent kinematic regions: The first term $n_L(x)$ is the triple-Regge term (see Fig. 2) which dominates near $x \approx 1$. While the second term gives the pionization contribution. Since in each term of the iteration series above, all Reggeon links have large rapidity separation, the multiperipheral configuration comes out.

(c) In obtaining (1) we have used the factorization property⁷ of multi-Regge diagrams. We have neglected the off-shell effect for the Reggeon-particle collision. This neglect is valid under our circumstances that non-canonical amplitudes are strongly suppressed.

(d) We need not introduce the usual lower cutoff,

$$dx/x \rightarrow dx/(x^2 + \mu^2/s)^{1/2},$$

in the integral in (1) and (2), because of the above property, $n_L(x) \rightarrow 0$ for $x \rightarrow 0$.

The behavior of $n_L(x)$ for $x \approx 1$ is obtained by the triple-Regge formula⁷

$$n_L^{(i)}(x) = \int dP_1^2 \frac{E}{\sigma^{\text{inel}}} \frac{d\sigma_L}{dP^3} = \int dP_1^2 \Gamma(t) \left[\frac{s}{M^2} \right]^{2\alpha(t)} \frac{\lambda(M^2)}{\lambda(s)} \frac{\sigma_i(M^2)}{\sigma_i(s)}, \quad (3)$$

where for the flux factor, $\lambda(M^2)/\lambda(s) \sim M^2/s$, $\Gamma(t)$ is the residue function and $\alpha(t)$ the trajectory of the internal Reggeon. This is the ordinary formula if we use $\sigma(M^2) \sim C(M^2)^{\alpha_p - 1}$. We assume for the total cross section that $\sigma_T = \sigma_P + \sigma_R = as^{\epsilon_T} + bs^{\epsilon_R}$. Here ϵ 's will be determined by the self-consistency condition as shown later.

In the infinite-momentum frame, (3) is reduced to the form⁷

$$n_L^{(i)}(x) = \gamma(x) (1-x)^{1-2\alpha+\epsilon_i}. \quad (4)$$

According to the convention of the one-dimensional model, α is identified with the Reggeon intercept $\alpha = \alpha(0)$. However, this may not be practically so good an approximation. There are suggestions that $\alpha < \alpha(0)$.^{8,9} We shall again come back to this problem in Sec. IV. Theoretically, the case $\alpha = \alpha(0)$ leads the interesting Reggeon bootstrap which gives the Pomeron with $\alpha_p(0) = 1$.

As mentioned before, $n_L(x) \rightarrow 0$ for $x \rightarrow 0$. Therefore, $\gamma(x)$ has the same property. Here we assume simple behavior⁷ $\gamma(x) \propto x^\delta$ and provide the following function over all x regions:

$$n_L^{(i)}(x) = A^{(i)} x^{\delta_i} (1-x)^{\beta_i}, \quad (5)$$

$$\beta_i \equiv 1 - 2\alpha + \epsilon_i, \quad \delta_i > 0.$$

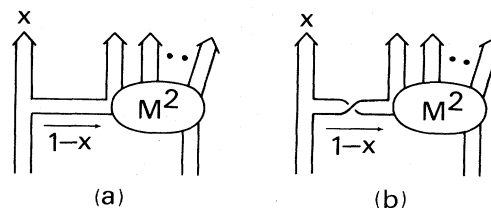


FIG. 3. The "uncrossed" diagram (a) and the "crossed" diagram (b) which correspond to $n_{L_u}(x)$ and $n_{L_c}(x)$, respectively.

$A^{(i)}$ is determined by the normalization condition (2). We determine the values of δ_i as follows. In the DMB model, $n_L^T(x)$ gets the contributions from the two diagrams in Fig. 3, but $n_L^R(x)$ only from one (uncrossed) of them. They have the same (left) vertex, and thus, $\delta_p = \delta_R = \delta$,

$$n_L^T(x) = 2g^2 x^\delta (1-x)^{\beta_T}, \quad n_L^R(x) = g^2 x^\delta (1-x)^{\beta_R}, \quad (6)$$

for which (2) gives the relations

$$2g^2 B(\delta, \beta_T + 1) = g^2 B(\delta, \beta_R + 1) = 1, \quad (7)$$

where $B(i, j)$ is the beta function. When we take $\delta = 1$, (7) is reduced to the famous Lee-Veneziano relation¹ which is the characteristic of the one-dimensional DTU, i.e.,

$$\begin{aligned} \epsilon_T &= \alpha_p - 1 = 2(\alpha - 1) + 2g^2, \\ \epsilon_R &= \alpha_R - 1 = 2(\alpha - 1) + g^2, \end{aligned} \quad (8)$$

where we have used the relations between ϵ_i and the output Pomeron or Reggeon intercept. The (bare) Pomeron intercept $\alpha_p = 1$ is derived from (8) by the familiar bootstrap condition $\alpha = \alpha_R$. If $\delta \neq 1$, we would get complicated nonlinear relations among α , g^2 , and ϵ_i . Whence one knows that DMB model corresponds to the special case $\delta = 1$.⁷ In what follows, we use the forms (6) with $\delta = 1$.

By means of the Mellin transformation,⁶

$$\tilde{n}^{(i)}(J) \equiv \int_0^1 dx x^{J-2} n^{(i)}(x), \quad (9)$$

we can solve the integral equation (1) and get

$$\tilde{n}^{(i)}(J) = \frac{\tilde{n}_L^{(i)}(J)}{1 - L^{(i)}(J)} \quad (10)$$

together with

$$\tilde{n}_L^{(i)}(J) = (\beta_i + 1) B(J, \beta_i + 1), \quad (11)$$

and

$$\begin{aligned} L^{(i)}(J) &= \int_0^1 (dx/x) (1-x)^{J-1} n_L^{(i)}(x) \\ &= (\beta_i + 1) / (J + \beta_i). \end{aligned} \quad (12)$$

Here we have used (6) and (8). Now the inverse transformation of (10) leads to

$$n^{(i)}(x) = (\beta_i + 1) (1-x)^{\beta_i} \quad (\beta_T = 2g^2 - 1, \beta_R = g^2 - 1). \quad (13)$$

The momentum sum rule $\tilde{n}^{(i)}(2) = 1$ can be readily obtained⁶: From (11) and (12), one gets $L^{(i)}(2) = \tilde{n}_L^{(i)}(1) - \tilde{n}^{(i)}(2)$. Insert this into (10) with $J = 2$ and use the normalization condition (2) [i.e., $\tilde{n}_L^{(i)}(1) = 1$], then we have $\tilde{n}^{(i)}(2) = 1$.

Recent experiments suggest the importance of the role of the valence quarks. In the final state, the mesons which are bound states of a "valence" and a "sea" parton are found uniquely in each DTU diagram. One of them is the

leading particle and the other the meson with asterisk (*) in Fig. 1. The behavior of the leading particle is described by $n_L(x)$. The corresponding quantity for the (*) meson, referred to as $n_v(x)$, satisfies the integral equation

$$\begin{aligned} n_v(x) &= \int_0^{1-x} (dy/y) n_{Lc}(y) n_L^T \left[\frac{x}{1-y} \right] \\ &\quad + \int_0^{1-x} (dy/y) n_{Lu}(y) n_v \left[\frac{x}{1-y} \right], \end{aligned} \quad (14)$$

where we have written the contributions from Fig. 3(a) and 3(b) separately as ($u \equiv$ uncrossed and $c \equiv$ crossed),

$$n_L^T(x) = n_{Lu}(x) + n_{Lc}(x) \quad \text{and} \quad (15)$$

$$n_{Lu}(x) = n_{Lc}(x) = g^2 x (1-x)^{\beta_T} \quad (2g^2 = \beta_T + 1).$$

Equation (14) is easily confirmed by the iteration. Taking the Mellin transform, we obtain

$$\tilde{n}_v(J) = \frac{\tilde{n}_L^T(J) L^T(J) / 2}{1 - (L^T(J) / 2)}, \quad (16)$$

and the inverse transformation of (16) leads to

$$\begin{aligned} n_v(x) &= [(\beta_T + 1) / 2] x (1-x)^{\beta_T + 1} \\ &\quad \times F(1, (\beta_T + 3) / 2; \beta_T + 2; 1-x) \end{aligned} \quad (17)$$

[$F(a, b; c; z)$ is the hypergeometric function]. Equation (16) satisfies the valence-number-conservation sum rule; $\tilde{n}_v(1) = 1$. For the mesons consisting of only sea quarks, we get

$$n_s(x) = n^T(x) - n_L^T(x) - n_v(x). \quad (18)$$

When $\alpha = \alpha_R = g^2 = \frac{1}{2}$ [the bootstrap solution of (8)], (13) and (17) become very simple, and we have

$$\begin{aligned} n^T(x) &= 1, \quad n_L^T(x) = x, \\ n_v(x) &= x^{1/2} (1-x)^{1/2}, \\ n_s(x) &= 1 - x^{1/2}, \end{aligned} \quad (19a)$$

and for the Reggeon sector,

$$n^R(x) = (\frac{1}{2}) (1-x)^{-1/2}. \quad (19b)$$

It is easily verified that the conventional formalism,¹ in terms of the rapidity integrals, of the one-dimensional DTU also gives the distributions (19a). Since (19a) satisfy the momentum sum rule the conventional formalism can accidentally, only in the case $\alpha = \alpha_R = g^2 = \frac{1}{2}$, give rise to the result consistent with the momentum conservation. Therefore one finds that in this case, our DMB formalism and the conventional one lead the same result.¹⁰ From (13) we obtain the cross section $xd\sigma/dx = \sigma_T \cdot n^T(x) = 2g^2 \sigma_T$ at $x = 0$. The conventional formalism also gives the same value for the cross section in the central region.¹ The rather trivial form $n^T(x) = 1$ in (19a) is the consequence of ignoring the quark flavors. In the

following sections, we take the flavors into account. In this case, the relative weights among n_L , n_v , and n_s terms become flavor dependent and thus nontrivial distributions emerge.

III. FLAVOR DEPENDENCE AND RESONANCE PRODUCTIONS

The introduction of the quark flavors into internal vertices is straightforward. Let g_{oo} , g_{os} , and g_{ss} be the coupling constants for producing a nonstrange, a strange, and a double strange ($q\bar{q}$) rung, respectively. A suppression factor F is introduced¹² for strange productions, i.e.,

$$g_{os}^2/g_{oo}^2 = g_{ss}^2/g_{os}^2 = F.$$

The flavor counting gives the following relations:

$$g^2 = 4g_{oo}^2 + 4g_{os}^2 + g_{ss}^2 = (2+F)^2 g_{oo}^2,$$

and thus

$$\begin{aligned} g_{oo}^2 &= g^2/(2+F)^2, & g_{os}^2 &= g^2 F/(2+F)^2, \\ g_{ss}^2 &= g^2 F^2/(2+F)^2. \end{aligned} \quad (20)$$

The production rate of the (q_i, \bar{q}_j) rung with the specific flavor (i, j) is easily obtained by multiplying $n_i(x)$ [(15), (17), and (18)] by g_{ij}^2/g^2 . Note that the suppression factor should not be introduced to the strange *valence* quark.

On the other hand, it is hard to take into account the differences among strange- or nonstrange-trajectory intercepts. In view of the smallness of F , the contributions from strange Reggeons is unimportant, except for the first or last link being attached to the end vertices in Fig. 1. When we consider the triple-Regge region ($|x| \cong 1$), the first (or last) link gets a large rapidity separation and gives sensitive effects to the leading-particle distribution. We therefore follow the prescription that for the first (last) one or two links, we consider the fact, $\alpha_\rho(0) \neq \alpha_{K^*}(0) \neq \alpha_\phi(0)$, while for all other links, we use the same value α . The calculations under this prescription can be easily

carried out by using the iterative property in Eqs. (1) and (14). For the kernels $n_L^T(y)$, $n_{Lc}(y)$, and $n_{Lu}(y)$ in these equations, we provide the corresponding intercepts $\alpha_i(0)$ ($i = \rho, K^*$, and ϕ) where $\alpha_\rho(0) > \alpha_{K^*}(0) > \alpha_\phi(0)$. And we do one or two iterations with the input functions given by (13), (15), and (17). These calculations have been done by computer and the result is shown in the next section.

The data suggest that a sizable part of meson production is through resonances.¹³ Hence, the rungs of the DM ladder represent not only stable mesons but also resonance states. In this paper, we will take the following simple picture:

(1) Only vector (nonet) mesons are considered with a production rate C (an adjustable parameter¹⁴) in a rung ($q\bar{q}$) state. For the (qqq) rung as the leading baryon in the proton fragments, we take the decuplet states with the (decuplet/octet) production ratio suggested by the SU(6) scheme.

(2) For simplicity, all resonance decays are treated as *two-body* decays with isotropic angular distribution in their rest system. This assumption would be reasonable because three-body decays are rare, except for ω . As for the *charged-pion* productions, our treatment would not lead to many errors coming from ω decay. For π^0 productions, it leads to about a 10% error in π^0 multiplicity.

(3) In two-body decay vertices, the $s\bar{s}$ pair productions are completely suppressed. Thus, we have no strange mesons from the decay of nonstrange ones.

Under these assumptions, we shall calculate various inclusive spectra: For example,

$$\begin{aligned} \frac{x}{\sigma} \frac{d\sigma}{dx}(\pi^+ \rightarrow h) &= \frac{1}{2} G_u^h(x) + \frac{1}{2} G_d^h(x) \quad (h = \pi^- \text{ or } \pi^0) \\ \frac{x}{\sigma} \frac{d\sigma}{dx}(\pi^- \rightarrow h) &= \frac{1}{2} G_u^h(x) + \frac{1}{2} G_d^h(x) \quad (h = \pi^+, \pi^0), \end{aligned} \quad (21)$$

where the subscripts represent the valence quark which connects with the DM ladder. For the direct production of h , we have

$$G_u^{\pi^-}(x) = G_d^{\pi^-}(x) = G_u^{\pi^+}(x) = G_d^{\pi^+}(x) = \frac{1}{(2+F)^2} n_s(\rho, \rho; x), \quad (22)$$

$$G_u^{\pi^0}(x) = G_d^{\pi^0}(x) = G_u^{\pi^0}(x) = G_d^{\pi^0}(x) = \frac{1}{2(2+F)} n_L(\rho; x) + \frac{1}{(2+F)^2} [n_v(\rho, \rho; x) + (F/2)n_v(K^*, K^*; x) + n_s(\rho, \rho; x)], \quad (23)$$

where $n_v(i, j; x)$, $n_s(i, j; x)$, and $n_L(i; x)$ are the corresponding $n(x)$ functions for which the first and second links are specified by the i and j Reggeons, respectively, according to the above-mentioned prescriptions. The indirect productions are given by

$$\begin{aligned} G_u^{\pi^-}(x) &= G_d^{\pi^-}(x) = G_u^{\pi^+}(x) = G_d^{\pi^+}(x) \\ &= \frac{1}{2(2+F)} R_L(\rho; x) + \frac{1}{(2+F)^2} \{R_v(\rho, \rho; x) + 2R_s(\rho, \rho; x) + \frac{F}{2}[R_v(K^*, K^*; x) + R_s(\rho, K^*; x) + R_s(K^*, \rho; x)]\}, \end{aligned} \quad (24)$$

$$\begin{aligned}
G_u^{\pi^0}(x) &= G_d^{\pi^0}(x) = G_{\bar{u}}^{\pi^0}(x) = G_{\bar{d}}^{\pi^0}(x) \\
&= \frac{1}{2+F} [R_L(\rho; x) + (F/4)R_L(K^*; x)] \\
&\quad + \frac{1}{(2+F)^2} \{2[R_v(\rho, \rho; x) + R_s(\rho, \rho; x)] \\
&\quad + \frac{1}{2}F[2R_v(K^*, K^*; x) + R_v(\rho, K^*; x) + R_s(\rho, K^*; x) + R_s(K^*, \rho; x) + \frac{1}{2}FR_v(K^*, \phi; x)]\}. \quad (25)
\end{aligned}$$

Here

$$R_\alpha(i, j; x) = \int_x^1 \frac{dz}{z} n_\alpha(i, j; z) \gamma \left(\frac{x}{z} \right) \quad (26)$$

is the convolution by the resonance decay factor. For the isotropic decay of mesons, $\gamma(x)/x \cong 1$. The total contributions to G 's are written as

$$(G)_{\text{total}} = (1-C)(G)_{\text{dir}} + C(G)_{\text{ind}}. \quad (27)$$

The expressions for other inclusive cross sections are given in the Appendix. In the proton fragmentations, the end vertex has a coupling constant different from g^2 . However, this difference has no effect on $n(x)$, because $n(x)$ is normalized with the factor $(1/\sigma^{\text{inel}})$ and the end-coupling constant is canceled out. The isotropic decay of the decuplet state leads the decay factor,

$$\gamma(x)/x = \frac{\theta([1 - (m/m^*)^2] - x)}{1 - (m/m^*)^2}, \quad (28)$$

where for the typical case, m and m^* are the nucleon and $\Delta(1236)$ masses, respectively.

IV. COMPARISON BETWEEN THE THEORETICAL AND EXPERIMENTAL RESULTS

Our DMB model gives the correct triple-Regge formula (at $t=0$) for $x \cong 1$, where the first (last) Reggeon propagator of the DM ladder gets large rapidity separation. The result for $x \sim 1$ is thus very sensitive to the value of α in (4). The recent analyses⁹ of $\pi^\pm p \rightarrow \pi^0 X$ data in terms of the triple-Regge formula suggest a small value $\alpha_\rho^{\text{eff}}(0) \sim 0.2$ for the effective ρ intercept. We therefore provide, for the first (last) one or two links in our model, the following effective values of $\alpha_i(0)$ which are somewhat smaller than those expected from the Chew-Frautschi plot:

$$\begin{aligned}
\alpha_\rho^{\text{eff}}(0) &= 0.2, \quad \alpha_{K^*}^{\text{eff}}(0) = 0, \\
\alpha_\phi^{\text{eff}}(0) &= -0.2. \quad (29)
\end{aligned}$$

The first value was suggested by Ref. 9 and we assume a similar shift for others.

From the arguments, not in the one-dimensional approximation, of the multi-Regge model, we have a suggestion⁸ that the effective value of α for interior links should be also smaller than $\alpha(0)=0.5$. First, we argue what is emerged in our *one-dimensional* model by lowering α for all inside Reggeons. Two different situations come out according to whether we break the bootstrap condition $\alpha_R = \alpha$ for Eq. (8) or not: (a) We take $\alpha_R \neq \alpha$ but $\alpha_R = 0.5$. In this case, we get $\alpha_p > 1$ and multi-Pomeron exchanges

will become important. Clearly this case is outside of the scope of the present model. (b) We assume $\alpha_R = \alpha$ (then $\alpha_p = 1$), but now $\alpha_R < 0.5$. Our predicted high-energy behaviors of the cross sections in the Reggeon sector are different from the empirical ones. However, if we restrict ourselves to the high-energy limit, all these cross sections vanish and we still have the meaningful result. Therefore we always assume the bootstrap condition $\alpha_R = \alpha$ [case (b) in this paper. We should remark that the use of α^{eff} for the first and the second links lead no change for α_R and α_p .

At present, no quantitative argument on the shift of α for interior links exists. Furthermore, a part of this shift is caused by the off-shell effect which we have neglected. We will not therefore enter the mechanism of the shifts. Instead, this α is treated as a free parameter and the following four cases are considered: (i) Only at the first link, we use the effective value $\alpha=0.5$; (ii) similar to (i) but (29) is used also on the second link; (iii) the same as (ii) but we take a

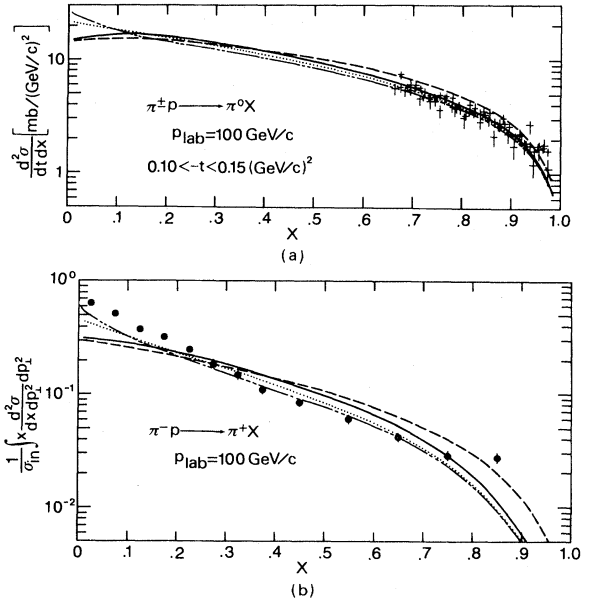


FIG. 4. Inclusive cross sections for the pion fragmentation: The dashed, solid, dotted, and dash-dot-dotted curves are calculated for the four cases, (i), (ii), (iii), and (iv) in the text, respectively. In (a), data (Ref. 9) on $\pi^\pm p \rightarrow \pi^0 X$ at small t are compared with our predictions (arbitrary normalization), while in (b), data (Ref. 15) on $\pi^- p \rightarrow \pi^+ X$ and our predictions are shown for the normalized cross section $n(x)$. [We use $\sigma^{\text{inel}}(\pi^- p) = 20.7$ mb at $E = 100$ GeV.]

smaller value $\alpha=0.2$ for interior links; and (iv) similar to (iii) but $\alpha=0$. From the above argument, it may be hard to think that case (iii) and (iv) are more faithful reflections of the true situation. Our aim for these cases is to see roughly how fragmentation spectra will change by the shift of α for interior links.

We calculate $\pi \rightarrow \pi X$ processes for these four cases. The $\pi^{\pm} \rightarrow \pi^0 X$ process is dominated by the triple-Regge (ρ - ρ - P) term for $x > 0.6$. Since we take the values in (29), all four cases show good agreements with the data [see Fig. 4(a)]. In $\pi^{-} \rightarrow \pi^{+} X$, only sea ($q\bar{q}$) productions are an important overall x region. Therefore, this process will be sensitive to the value of α for interior links. In Fig. 4(b), one sees that the disagreements with the data, seen in case (i) or (ii), are considerably reduced by lowering the value of α [(iii) and (iv)]. This is especially remarkable for small x . For $x > 0.3$, even case (ii) can give a rough explanation of the data. For $x \approx 0.05$ [which is larger than the lower cutoff μ/\sqrt{s} ($\mu \sim 0.3$ GeV)], the predicted cross section in the case (iv) is still smaller than the data about 40%. We shall find similar results in other pion productions [see Fig. 6(a)]. Since we are dealing with the normalized cross section, this means insufficient central π multiplicity in our model. We notice that case (iv) gives already too large ρ production at $x \approx 0$ as seen in Fig. 5. Therefore, it is hard to get the eventual agreement with the data at $x \approx 0$ by only the lowering of α .

In the above, we have taken $C=0.5$ in (27) and $F=0.2$.

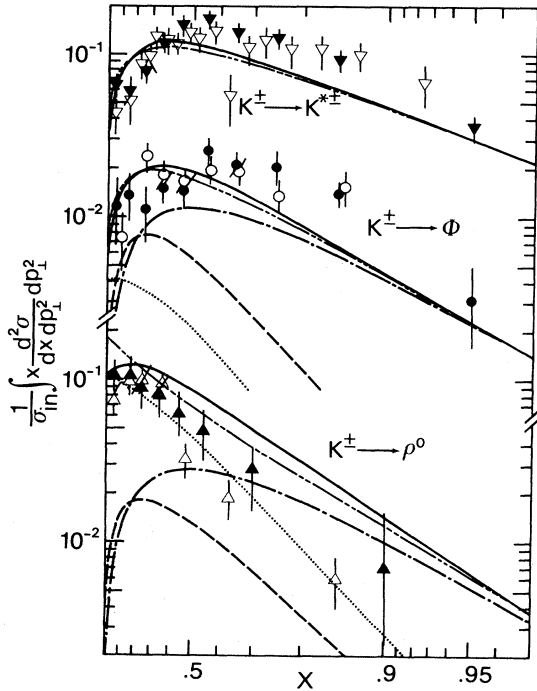


FIG. 5. Vector-meson production in K^{\pm} fragmentations: The dashed, dotted, and dash-dotted curves show, respectively, $n_s(x)$, $n_v(x)$, and $n_L(x)$ contributions in case (ii) in the text. The solid curves show the total contributions. While the dash-dot-dotted curve shows the total contribution in the case (iv). The open (closed) points correspond to $K^{+}+p$ ($K^{-}+p$) data (Ref. 16) normalized by $\sigma^{\text{inel}}(K^{+}+p)=15.3$ mb [$\sigma^{\text{inel}}(K^{-}+p)=18.0$ mb].

These values are determined by the analysis of the vector-meson productions given below. We have neglected tensor and axial-vector productions. The inclusion of these higher-resonance contributions will also increase the cross section for small x . In order to get a rough estimation for this, we consider the 30% increase of the vector production rate ($C=0.65$), which corresponds to the π multiplicity increase from the tensor production whose rate is about 20% of the vector's. This calculation gives only $\sim 18\%$ rise of the cross section at $x \approx 0.05$, which is not yet sufficient. This difficulty might be related to the effect from the breaking of the Feynman scaling which is not taken in our model. We do not discuss here the $\pi^{\pm} \rightarrow \pi^{\pm} X$ because in our model, the triple-Pomeron coupling is a higher-order (multiladder) configuration and could not be easily calculated.

Since we are dealing with the normalized cross section $(xd\sigma/dx)/\sigma$, the coupling constant for the end vertex is canceled out. Therefore, we have no free parameter which shifts the individual curves in Fig. 4(b) and Figs. 5 and 6, except for only two parameters C and F . One, however, sees that our overall normalization is excellent. This is because our model satisfies the longitudinal-momentum conservation. Indeed, the integration of $(xd\sigma/dx)/\sigma$ over x gives the momentum sum rule.

Now let us analyze the recent Serpukhov data¹⁶ on ρ^0 , K^{*} , and ϕ productions from $K^{\pm}+p$ collisions. The results are shown in Fig. 5, where the curves are calculated in

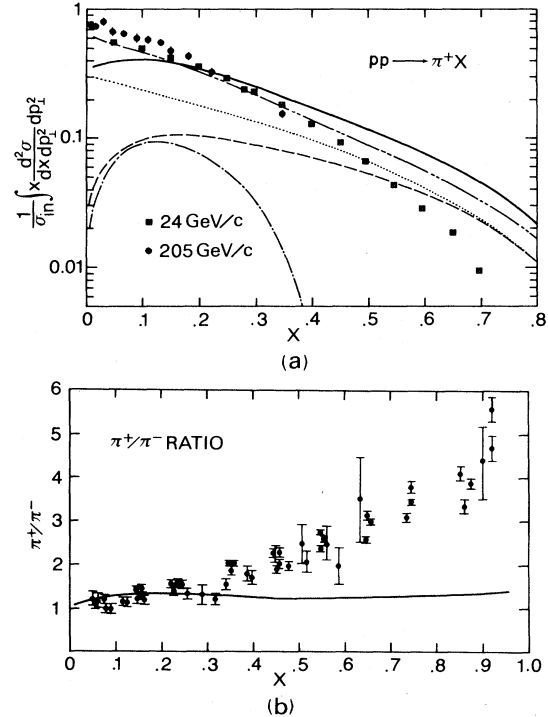


FIG. 6. The result for the proton fragmentation: (a) π^{+} distribution and (b) π^{+}/π^{-} ratio. The data are from Ref. 17. The solid, dotted, dashed, and dash-dotted curves in (a) are, respectively, the total, sea, valence, and $\Delta(1236)$ decay contributions in case (ii), while the dash-dot-dotted curve is the total contribution in case (iv). In (b) we show the result only for case (ii), since case (iv) gives the similar curve.

cases (ii) and (iv) mentioned above. Normalizations of individual curves depend on the choices of C and F . In case (ii), $F=0.2$ and $C=0.5$ lead the best fit (the solid curves in Fig. 5) to the cross sections near $x \approx 0$, and these values are consistent with the results of previous analyses² in the central region. For $x < 0.5$ we get rather successful results but some disagreement is found for $x > 0.5$. One finds for $x \sim 1$ that the effective values for $\alpha_p(0)$ and $\alpha_{K^*}(0)$ given in (29) give rise to the correct slopes for the $K \rightarrow \phi$ and $K \rightarrow K^*$ cross sections, but the predicted magnitudes for $x > 0.6$ are somewhat smaller than the data. The $K \rightarrow \rho^0$ data show steeper decreasing than the $K \rightarrow \phi$ case. However, these two processes are dominated by the same triple-Regge (K^*-K^*-P) configuration and thus our model gives the same slope. This disagrees with the data. Note that we have no addition parameter. It is worth noticing that in the recombination model,⁴ this difference in slopes is attributed to the different momentum distributions of the strange or the nonstrange valence quarks in the incident K . Our DMB model as well as other conventional Regge models have no room for taking valence distributions into account. Hybrid models between parton and Regge formalisms might be interesting. The lowering of α for interior links does not lead to any improvement for the vector productions. The shoulder at small x seen in $K^\pm \rightarrow \rho^0$ disappears (see Fig. 5).

For the proton fragmentations, our DMB model has severe difficulties. In Fig. 6(a), we show our prediction for $p \rightarrow \pi^+ X$. The solid [dash-dot-dotted] curve represents, in case (ii) [(iv)], the sum of the contributions from sea- and valence- $(q\bar{q})$ (in the $*$ position in Fig. 1) rungs and also from the decuplet $\Delta(1236)$ decays at the end vertex. We have no triple-Regge (BBP -type) terms, because baryon exchanges have been neglected in our model. We find that our sea contribution is again insufficient to reproduce the data at $x \approx 0$. The situation is very similar to the $\pi^- \rightarrow \pi^+$ case discussed before. On the other hand, we get too large a cross section for $x > 0.5$, which is approximately represented by $\sim(1-x)^{1.6}$. This large cross section is the reflection of our choice $\delta=1$ in (6), because it comes from the configurations where the strong ordering is broken. Can we improve the situation if we take the triple-Regge term into our consideration? The answer is no. Because, the power 1.6 above is nearly equal to or less than the power $1-2\alpha_N$ of the triple-Regge (NNP) term [if we take the value of the neutron intercept, $\alpha_N(0)=(-0.35) \sim (-0.65)$] and thus the NNP term cannot be the dominant term in the region $x \approx 1$. We note that in the analysis¹⁸ of $p \rightarrow \pi^\pm X$ by the triple-Regge terms, we find the curious result $-\alpha_\Delta(0) < \alpha_N(0)$.

Another difficult problem is the positive-negative particle ratios (π^+/π^- or K^+/K^-). As seen in Fig. 6(b), we could not predict the large increase in $x > 0.5$, shown by the data. We get a similar result for K^+/K^- .¹⁹ In the recombination model,⁴ this increase is attributed to the effect of the valence quark which is recombined into a fast meson, and the above particle ratios are correlated to the abundance of the fast u/d valence quarks in the proton. In our model, this region ($x > 0.5$) is dominated by the sea and valence $(q\bar{q})$ contributions as discussed above. The sea contribution is charge symmetric. Since our end vertex is the usual baryon-baryon-Reggeon coupling, where the baryon is treated as if the elementary, our valence term

is flavor independent except for its normalization depending on the quark counting. The valence effect in our model is so weak that it could not change the particle ratio so much. In order to overcome this trouble, we would need to modify the end vertex so that we can get a more explicit role from the constituent structure of the incident hadron.

V. SUMMARY

In the previous sections, we have extended the bootstrap multi-Regge formalism given in Ref. 7 to include the quark flavors in the framework of the DTU scheme. Flavor-dependent inclusive spectra of various processes are obtained by extracting the leading, valence, and sea terms separately. We obtained good agreement between the theoretical and experimental spectra for the vector productions for $x < 0.5$ (Fig. 5), where no ambiguities from the decay process occur. This means that the theory is successful in the following two points.

- (1) The predicted relative strengths among the above three terms.
- (2) The small- x behavior of the leading and valence terms.

We note that (1) is the direct consequence of the DTU scheme (the flavor counting plus the choice of the parameter F), while (2) is the reflection of our choice $\delta=1$ in Eq. (5), which corresponds to the Lee-Veneziano relation (8), i.e., the characteristic feature of the one-dimensional model.

In spite of these facts, we have encountered many difficulties, such as the following.

- (a) Insufficient pion multiplicity for $x \approx 0$, with $\alpha = \alpha_R = \frac{1}{2}$ and $\alpha_p = 1$.
- (b) Equal slopes for $x > 0.6$ in the $K^\pm \rightarrow \rho^0$ and ϕ productions.
- (c) The pion spectra or π^+/π^- ratio in the proton fragmentation for $x \sim 1$.

For (a), considerable improvement is expected by taking smaller α values for interior links. More elaborate estimations of the contributions from higher-mass resonance decay are also interesting. Recent data shows the energy dependence of the pion production at $x \approx 0$, which means the breakdown of the Feynman scaling. Our model satisfies Feynman scaling. Therefore, the mechanism for the scale breaking (for instance, the multi-Pomeron exchange) may give new contributions which may resolve the difficulty. (The normalization of the vector productions at $x \approx 0$ can be readjusted by choosing appropriate value of C .) Consistent formalism of such a model cannot be, however, obtained in the framework of the one-dimensional model as already discussed. The difficulties (b) and (c) might be related to the details of the valence structure of the incident hadrons as already pointed out. More elaborate end-vertex function must be provided. However, we have no room for doing this in our one-dimensional Regge model. Therefore, further developments of the bootstrap formalism by taking the transverse freedom (not one-dimensional) are very interesting, and detailed explorations of the end-vertex functions are important.

ACKNOWLEDGMENT

We would like to thank Dr. E. Takasugi for reading of the manuscript and critical discussions on the presentation.

APPENDIX

Here we give the expressions of some inclusive cross sections. For vector productions from K^+ ;

$$G_u^\phi(x) = F[\eta n_L(K^*) + Fn_s(K^*, K^*)]/\eta^2,$$

$$G_s^\phi(x) = F[2n_v(K^*, K^*) + Fn_v(\phi, \phi) + Fn_s(\phi, \phi)]/\eta^2,$$

$$G_u^{K^{*+}}(x) = \{\eta n_L(\rho) + F[2n_v(\rho, K^*) + Fn_v(K^*, \phi) + n_s(K^*, \rho)]\}/\eta^2,$$

$$G_s^{K^{*+}}(x) = [\eta Fn_L(\phi) + 2n_v(K^*, \rho) + Fn_v(\phi, K^*) + Fn_s(K^*, \phi)]/\eta^2,$$

$$G_p^0(x) = [2n_v(\rho, \rho) + Fn_v(K^*, K^*) + 2n_s(\rho, \rho)]/(2\eta^2),$$

$$G_s^0(x) = [\eta n_L(K^*) + 2n_s(K^*, K^*)]/(2\eta^2).$$

And for π productions from the proton:

$$\frac{x}{\sigma} \frac{d\sigma}{dx}(p \rightarrow \pi^\pm) = \frac{2}{3} G_u^{\pi^\pm} + \frac{1}{3} G_d^{\pi^\pm},$$

where (direct production)

$$G_u^{\pi^+} = G_d^{\pi^-} = [2n_v(\rho, \rho) + Fn_v(K^*, K^*) + n_s(\rho, \rho)]/\eta^2,$$

$$G_u^{\pi^-} = G_d^{\pi^+} = n_s(\rho, \rho)/\eta^2,$$

(indirect production)

$$G_u^{\pi^+} = A + B, \quad G_d^{\pi^-} = B \quad \text{and} \quad G_u^{\pi^-} = A + C,$$

$$G_d^{\pi^+} = (15\eta)^{-1}[19R_L(\rho) + 4FR_L(K^*)] + C,$$

with

$$A \equiv (45\eta)^{-1}[12R_L(\rho) + 5FR_L(K^*)],$$

$$B \equiv (2\eta^2)^{-1}[6R_v(\rho, \rho) + 2FR_v(\rho, K^*) + 3FR_v(K^*, K^*) + F^2R_v(K^*, \phi) + 4R_s(\rho, \rho) + FR_s(\rho, K^*) + FR_s(K^*, \rho)],$$

and

$$C \equiv (2\eta^2)^{-1}[2R_v(\rho, \rho) + FR_v(K^*, K^*) + 4R_s(\rho, \rho) + FR_s(\rho, K^*) + FR_s(K^*, \rho)].$$

In the above, we have used the abbreviations $n_v(i, j) \equiv n_v(i, j; x)$, etc., and $\eta = 2 + F$.

¹H. Lee, Phys. Rev. Lett. **30**, 719 (1973); G. Veneziano, Phys. Lett. **52B**, 220 (1974); Nucl. Phys. **B74**, 365 (1975).

²H. M. Chan, J. E. Paton, and S. T. Tsou, Nucl. Phys. **B86**, 13 (1975); N. Papadopoulos, C. Schmid, C. Sorensen, and D. M. Webber, *ibid.* **B101**, 189 (1975); M. Fukugita, T. Inami, N. Sakai, and S. Yazaki, Phys. Rev. D **19**, 187 (1979); Chung-I. Tan, *ibid.* **22**, 1024 (1980); and more complete references are seen in the last two papers.

³A. Capella, U. Sukhatme, C. I. Tan, and J. Trân Thanh Vân, Phys. Lett. **81B**, 68 (1979); G. Cohen-Tannoudji, A. El Hassouni, J. Kalinowski, and R. Peschanski, Phys. Rev. D **19**, 3397 (1979).

⁴W. Ochs, Nucl. Phys. **B118**, 397 (1977); K. P. Das and R. C. Hwa, Phys. Lett. **68B**, 459 (1977); D. W. Duke and F. E. Taylor, Phys. Rev. D **17**, 1788 (1978); E. Takasugi, in *Proceedings of the XIth International Symposium on Multiparticle Dynamics, Bruges, 1980*, edited by E. De Wolf and F. Verbeure (University of Antwerp, Antwerp, Belgium, 1980).

⁵W. Kittel, in *Proceedings of the Xth International Symposium on Multiparticle Dynamics, Goa, India, 1979*, edited by S. N. Ganguli, P. K. Malhotra, and A. Subramanian (Tata Institute, Bombay, 1980).

⁶A. Krzywicki and B. Petersson, Phys. Rev. D **6**, 924 (1972); J. Finkelstein and R. D. Peccei, *ibid.* **6**, 2606 (1972).

⁷R. J. Yaes, Phys. Rev. D **10**, 941 (1974); **12**, 805 (1975).

⁸U. Sukhatme, C.-I. Tan, and J. Trân Thanh Vân, Z. Phys. C **1**, 95 (1979); C.-I. Tan, and D. M. Tow, Phys. Lett. **53B**, 452 (1975); J. Kwiecinski and N. Sakai, Nucl. Phys. **B106**, 44 (1976).

⁹A. V. Barnes *et al.*, Nucl. Phys. **B145**, 45 (1978).

¹⁰In order that the momentum conservation is satisfied in the

conventional formalism, we have to insert the delta function $\delta(1 - \sum_{k=1}^n x_k)$ into the ordered rapidity integrals [$x_k \equiv \exp(y_k - y_{\max})$]. The estimation of the integrals becomes extremely difficult. But for the special case $\alpha = \alpha_R = g^2 = \frac{1}{2}$, $(x_n/x_1)^{2\alpha-1} = 1$ and we can evaluate the integrals by using the formulas given in Ref. 11, and we find the same result as (19a) again.

¹¹K. Hirose and T. Kanki, Prog. Theor. Phys. **65**, 1391 (1981).

¹²N. Papadopoulos, C. Schmid, C. Sorensen, and D. M. Webber, Nucl. Phys. **B101**, 189 (1975).

¹³P. V. Chliapnikov *et al.*, Nucl. Phys. **B176**, 303 (1980).

¹⁴Here we do not take the SU(6) scheme. Instead, C is determined by the fit of vector-production data. Experimentally the tensor-production rate is substantially smaller than the vector. We neglect tensor productions and the remainder is identified with pseudoscalar mesons. A rung (q, \bar{q}) state in the DM ladder must include the charge-conjugation-even and -odd states in equal weight. The value $C \sim 0.5$ we found is consistent with this property of the rung.

¹⁵A. K. Nandi *et al.*, Nucl. Phys. **B169**, 20 (1980).

¹⁶D. Denegri *et al.*, Phys. Lett. **98B**, 127 (1981); C. Cochet *et al.*, Nucl. Phys. **B155**, 333 (1979); P. V. Chliapnikov *et al.*, *ibid.* **B176**, 303 (1980).

¹⁷V. Blobel *et al.*, Nucl. Phys. **B69**, 454 (1974); T. Kafka *et al.*, Phys. Rev. D **16**, 1261 (1977); J. R. Johnson *et al.*, *ibid.* **17**, 1292 (1978).

¹⁸J. Singh *et al.*, Nucl. Phys. **B140**, 189 (1978).

¹⁹K. Hirose and T. Kanki, in *Proceedings of the XII International Symposium on Multiparticle Dynamics, Notre Dame 1981*, edited by W. D. Shephard and V. P. Kenney (World Scientific, Singapore, 1982).